Limnology and Oceanography
FLUIDS & ENVIRONMENTS

ORIGINAL ARTICLE

Simultaneous field measurements of ostracod swimming behavior and background flow

K. R. Sutherland,[1,2] **J. O. Dabiri,**[3] **and M. A. R. Koehl**[4]

Abstract

Zooplankton swimming near the substratum experience boundary layer flow that is characterized by steep velocity gradients and turbulence. How do small swimming organisms navigate flows at this interface to forage and interact with mates? To address this question, we collected field measurements of the swimming behavior of the marine ostracod Paravargula trifax *near complex living substrata, which were exposed to two conditions: slow "ambient flow" and faster "experimental flow." Ostracod trajectories and background flow were recorded simultaneously using a self-contained underwater velocimetry apparatus (SCUVA). Particle image velocimetry (DPIV) produced instantaneous velocity vector fields in which the ostracods were swimming. Mean velocities, local shear stresses, turbulence intensity, and boundary shear velocity (u_*) were greater in the experimental flow treatment. In slow ambient flow ($u_{rms} = 0.39 \pm 0.13$ [mean $\pm$ SD] cm s^{-1}), ostracod swimming tracks were more tortuous and swimming angles corrected for background flow were randomly distributed compared with tracks in faster flow ($u_{rms} = 3.49 \pm 0.50$ cm s^{-1}), indicating decreased maneuverability in rapidly flowing, turbulent water. Modeled, passive neutrally buoyant particles moved at substantially slower speeds, and their tracks were less tortuous than those of the ostracods, thus illustrating the importance of behavior as well as environmental flow in determining ostracod trajectories. Frequencies of encounters by ostracods with the benthos and with other ostracods were not different between treatments. However, in the experimental flow treatment, interactions with other ostracods occurred more frequently in the boundary layer than in the free stream, suggesting that microhabitats in the boundary layer may allow for enhanced mating encounters.*

Keywords: benthic boundary layer, *Paravargula trifax*, SCUVA, shear, zooplankton

[1]Bioengineering, California Institute of Technology, Pasadena, California 91125, USA

[2]Current address: Institute of Ecology and Evolution and Oregon Institute of Marine Biology, 5289 University of Oregon, Eugene, OR 97403, USA

[3]Graduate Aeronautical Laboratories, California Institute of Technology, Pasadena, California 91125, USA

[4]Department of Integrative Biology, University of California, Berkeley, California 94720, USA

Correspondence to
K. R. Sutherland
ksuth@uoregon.edu

Introduction

[1] Locomotory behavior of freely swimming marine zooplankton has been the subject of numerous investigations. Specifically, in order to understand the kinematics of swimming and the propulsive forces generated by the organisms, some studies have tracked the movements of plankton in still water tanks (e.g., Zaret and Kerfoot 1980; Williams 1994). Conversely, in an effort to study the underlying effects of background flow on swimming behavior, other studies have investigated movements of zooplankton in steady, flume flow (e.g., Butman et al. 1988; Woodson et al. 2005) and in turbu-

lence tanks with oscillating grids (Saiz and Kiørboe 1995; Fuchs et al. 2004) or with intermittent jets (Yen et al. 2008). More recently, efforts have been made to construct individual-based models based on behavioral responses to environmental cues in realistic turbulent environmental flows (Koehl et al. 2007).

[2] Despite considerable progress toward understanding the interplay between zooplankton behavior and moving fluids, laboratory studies and models have inherent limitations due to experimental artifacts such as organisms bumping into the laboratory apparatus, imperfect replication of field flow conditions in the laboratory, and the simplification of model parameters. Furthermore, there are few studies of the effects of ambient water flow on animal swimming in the natural environment because of the difficulty of simultaneously tracking the motions of tiny organisms and the background flow environment. In short, we lack a complete understanding of the influence of realistic flows on the trajectories of zooplankton swimming in the natural environment.

[3] Marine organisms that are concentrated at the benthic boundary layer live at an interface that is often characterized by topographic complexity as well as complex water flow and steep velocity gradients that vary in space and time as tides and weather conditions change (e.g., Nowell and Jumars 1984). Freely swimming organisms associating with the benthos, including meroplankton and holoplankton, therefore face a wide range of water movement, from very slow flow in the interstices between adult benthic organisms to the free-stream velocity at some distance above the benthos. This complex fluid environment structures the ecological interactions of the resident zooplankton by influencing predation (Robinson et al. 2007), feeding rates (Saiz and Kiørboe 1995), and fecundity (Irigoien et al. 2000).

[4] The nonluminescent myodocopid ostracod *Paravargula trifax* Kornicker provides an excellent model system in which to examine zooplankton interactions with fluid dynamics because ostracods are ubiquitous in marine environments, ranging from tidal pools to the deep sea; most species are associated with benthic habitats and play an important role in benthic–pelagic coupling (Marcus and Boero 1998). Benthic species of myodocopid ostracods are known to spend daylight hours associated with sessile benthic communities or buried in the sediment, emerging at twilight in response to a critical "dark threshold" (Gerrish et al. 2009) and performing transitory displays in the water column until dawn (Rivers and Morin 2008, 2009). Myodocopid ostracods are omnivores, feeding on live prey and algal material, as well as scavenging dead organisms (Vannier et al. 1998). Although laboratory experiments have demonstrated that bioluminescent myodocopid ostracods exhibit complex swimming behavior during courtship, little is known about behaviors of nonluminescent species under natural field conditions (Rivers and Morin 2008, 2009).

[5] Our objective was to investigate the swimming motions of *P. trifax* in relation to the flow environment in the benthic boundary layer in the field. In so doing we examined: (1) how individual swimming trajectories are influenced by local flow; (2) how swimming orientation is influenced by water velocity and shear; and (3) to what extent ecological interactions (i.e., interactions with the benthos and with other ostracods) are modulated by the flow environment.

Methods

Field Data Collection

[6] Flow measurements and ostracod swimming tracks were collected under a floating dock in Kanehoe Bay, Oahu, Hawaii, during August 2009 using a self-contained underwater velocimetry apparatus (SCUVA) (Katija and Dabiri 2008). SCUVA is a compact, fully submersible instrument for collecting digital particle image velocimetry (DPIV) measurements in the field (Fig. 1). Ambient particles (0.01–0.1 mm) and ostracods (1–3 mm) in the water column were illuminated by a 1-mm-thick laser light sheet produced by a continuous 658-nm (red) 550-mW laser diode (Orion model; Laserglow Technologies, Canada), and the motion of these particles was imaged using a high-resolution video camera (model HDR-HC9 1440 × 1080 pixels, 30 fps; Sony, Japan) in an underwater housing (Bluefin Pro model; Light and Motion, USA). The density of ambient particles in the shallow coastal lagoon was sufficient for DPIV. In DPIV, the average displacement of a group of particles between successive images is computed via cross-correlation to produce a velocity

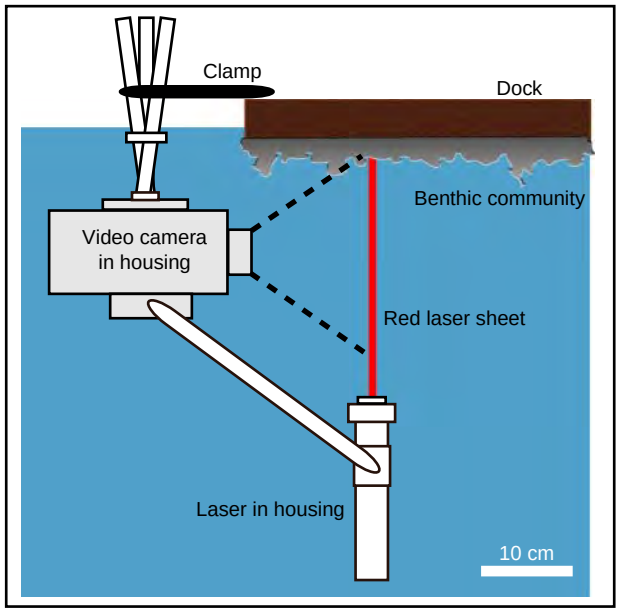

Fig. 1 Side-view schematic of SCUVA setup under floating dock in Kanehoe Bay, Oahu, Hawaii. Dashed lines indicate the camera field of view; scale bar is shown at the lower right. The direction of flow in the experimental flow treatment is into the page. Note that the dock extends beyond the diagram to the right.

vector map (Adrian 1991; Willert and Gharib 1991). Further details of a similar version of SCUVA are provided in a recent publication (Katija and Dabiri 2008).

[7] SCUVA was attached to a tripod and then affixed, upside down, to the long edge of the 5×2 m dock at a distance of approximately 2 m from the upstream end of the dock so that the laser sheet illuminated a two-dimensional slice of the benthic community under the dock as well as the adjacent seawater (Fig. 1). The field of view was approximately 10×12 cm. Data were collected at twilight, when ostracods were active in the water column and there is sufficient contrast between particles and background. Two flow conditions were measured: (1) "ambient flow," the natural fluid motion under the stationary dock, and (2) "experimental flow," the fluid motion produced by pulling the floating dock at a constant velocity such that the direction of the flow relative to the dock was parallel to the laser sheet for SCUVA imaging. An operator on shore pulled the dock horizontally using a rope attached to the upstream end of the dock; this is equivalent to flow past a stationary dock due to Galilean invariance of the reference frame.

[8] To verify that ostracods were present, a snorkeler conducted a plankton tow under the dock several centimeters below the benthic community using a handheld ring net (100 μm mesh size). Plankton samples examined under a dissecting microscope were dominated by a single species of ostracod, identified as *Paravargula trifax*. A representative sample was archived at the Smithsonian National Museum of Natural History (transaction no. 2052903).

Flow Characterization

[9] Image pairs collected with SCUVA were processed using a custom, cross-correlation DPIV algorithm (courtesy of M. Gharib, California Institute of Technology) with an interrogation window size of 32×32 pixels and a 50% overlap. A postprocessing step removed outliers that were more than three times greater than neighboring vectors and replaced them by interpolating between neighboring vectors; this procedure successfully removed the motion of the ostracods. The resultant instantaneous velocity vector maps were processed using MATLAB (Mathworks, USA) to quantify several flow parameters in the x–z plane, where x is parallel to the dock (horizontal) and z is orthogonal to the dock (vertical). Each variable was calculated spatially, across the two-dimensional flow field, and temporally, across time steps. The computed flow measurements included the u velocity in the x-direction, the w velocity in the z-direction, speed ($s = \sqrt{u^2 + w^2}$), and speed shear rate, γ, calculated as

$$\gamma = \sqrt{\left(\frac{\partial s}{\partial x}\right)^2 + \left(\frac{\partial s}{\partial z}\right)^2}. \quad (1)$$

The root-mean-square velocity in the x and z directions, u_{rms} and w_{rms}, respectively, were calculated as the spatially averaged root-mean-square velocity over all time steps. As a second measure of the velocity gradient, the boundary shear velocity, u_*, was calculated following the law of the wall:

$$u(z) = \frac{u_*}{\kappa} \ln \frac{z}{z_0}, \quad (2)$$

where $u(z)$ is the time-averaged velocity above the substratum at vertical distance z from the substratum, z_0 is

the roughness length of the substratum, and κ is von Kármán's constant ($\kappa = 0.41$) (Denny 1988). Two replicates of the ambient flow treatment and three replicates of the experimental flow treatment from the same evening were combined because the flow condition did not differ between replicates. The total numbers of time steps used in the calculation of flow parameters were 428 in the ambient condition and 629 in the experimental flow condition (14.3 and 21.0 s), which represent the total durations of the video sequences in which the rapid behavioral responses of the ostracods were measured.

Swimming Behavior

[10] Ostracod positions were digitized manually in ImageJ (National Institutes of Health, USA) at each time step (0.033 s), until the individual exited the field of view, to produce swimming trajectories. Measured behavioral metrics, described in more detail below, included observed velocity, relative swimming velocity, net:gross displacement ratio (NGDR), swimming angle, number and position of encounters with the benthos, and number and position of encounters with conspecifics. For each of the velocity measurements, mean speed and direction were also calculated from the velocity vectors. Sample sizes were limited to ostracods that swam within the field of view; thus, sample sizes were small within each replicate. Therefore, we pooled the data from the two ambient flow replicates and the three experimental flow replicates for our analysis.

[11] Observed velocities measured directly from the video records represent the vector sum of the ostracod swimming velocity and the local fluid velocity. Relative swimming velocities at each time step were calculated using a MATLAB routine to subtract the velocity vector local to the ostracod, based on linear interpolation from neighboring points, from the observed ostracod velocity vector. The NGDR, which is the shortest distance between the start and end points of a trajectory divided by the total distance traveled (Dicke and Burrough 1988), was used to assess the straightness of the observed trajectories (a low NGDR indicates a trajectory with a high degree of tortuosity). The NGDR was then compared between treatments using a *t*-test, after transforming nonnormal data using an arcsine square root transform (appropriate for proportions) to assess whether flow condition influenced tortuosity of the swimming tracks. To test whether observed ostracod trajectories were the result of their behavior and physical properties (shape and density), rather than simply due to passive transport of their fluid environment, we tracked the paths that passive, neutrally buoyant particles would take through the same velocity field if they had the same initial positions as the tracked ostracods.

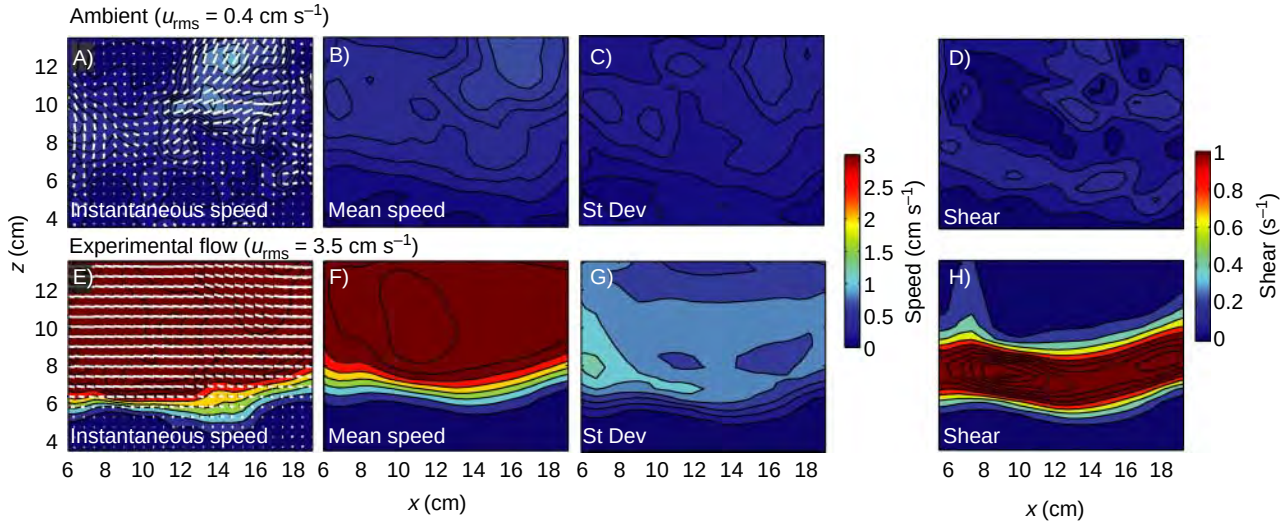

Fig. 2 Ambient (A–D) and experimental flow (E–H) conditions from DPIV data. Velocity vectors and contours of speed magnitude from a representative pair of video frames are shown in A and E. Mean speed (s) is shown in B and F, standard deviation in C and G, and shear rate (γ) contours in D and H (see text for details). The field of view has been rotated so that the substratum is at the bottom of the frame.

Table 1 Flow field characterization from DPIV data (mean ± SD). The boundary shear velocity, u_* (equation (2)), which describes the velocity gradient near the substratum, was calculated from a single vertical transect through the flow field; u_0 is the free-stream velocity. Shear rate, γ, was measured from the top of the substratum ($z \sim 5$ cm) to the top of the field of view ($z \sim 13$ cm). Shear rates in the lower ($z < 9$ cm) and upper ($z > 9$ cm) halves of the field of view are also reported to represent mean flow in the benthic boundary layer and in the free-stream flow, respectively.

					Shear rate, γ		
Flow condition	u_{rms} (cm s^{-1})	w_{rms} (cm s^{-1})	u_* (cm s^{-1})	u_0 (cm s^{-1})	**Total**	$z < 9$ cm	$z > 9$ cm
Ambient	0.39 ± 0.13	0.32 ± 0.06	0.04 ± 0.001	0.34 ± 0.04	0.09 ± 0.01	0.09 ± 0.01	0.09 ± 0.01
Experimental	3.49 ± 0.50	0.39 ± 0.13	1.11 ± 0.17	3.83 ± 0.13	0.60 ± 0.13	1.11 ± 0.20	0.22 ± 0.04

[12] Swimming angles were computed based on the u and w velocities at each time step ($\theta = \text{atan2}(u, w)$ in units of radians). Uniformity of instantaneous swimming angles pooled for all individuals based on relative swimming velocities (i.e., with background fluid motion subtracted) was analyzed for each treatment using Rayleigh's test (Zar 1999). Uniformity of mean swimming angles for each track was also analyzed for each treatment using Rayleigh's test. Interactions with the benthos and conspecifics were scored by viewing each frame and were defined as coming within one body length of the benthos or another ostracod, respectively. We computed numbers of interactions by dividing tracks into 0.5-s track intervals and counting the number of interactions in each interval. Numbers of interactions in each category were arranged in a contingency table. In each treatment, numbers of interactions with conspecifics in the boundary layer versus in the free-stream flow were compared using a χ^2 test, and z-positions of interactions (distance from the benthos) were compared using a Mann–Whitney rank sum test.

Results

Flow Field

[13] Instantaneous and time-averaged flow fields for the ambient and experimental flow treatments are shown in Fig. 2. The mean u_{rms} velocities in the ambient and experimental flow treatments measured over the entire. flow field were 0.39 ± 0.13 [mean ± SD] and 3.49 ± 0.50 cm s^{-1}, respectively. The standard deviations of the mean speed, s were higher in the experimental flow treatment, indicating more variable flow (Fig. 2C, G). The benthic boundary layer was defined as $z < 9$ cm based on the distance from the substratum where the velocity was 99% of the mean free-stream velocity in the experimental flow treatment. Plots of mean velocity and shear rate as a function of distance from the substratum (Fig. 2B, D, F, H) show a consistent increase in velocity with distance from the substratum in the benthic boundary layer and a constant velocity profile in the free-stream flow. Overall, the shear rate, γ, was approximately six times higher in the experimental flow treatment (Table 1; Fig. 2D, H). However, in the ambient flow treatment, shear rates were similar in the boundary layer ($z < 9$ cm) and in the free-stream flow ($z > 9$ cm), whereas, in the experimental flow treat-

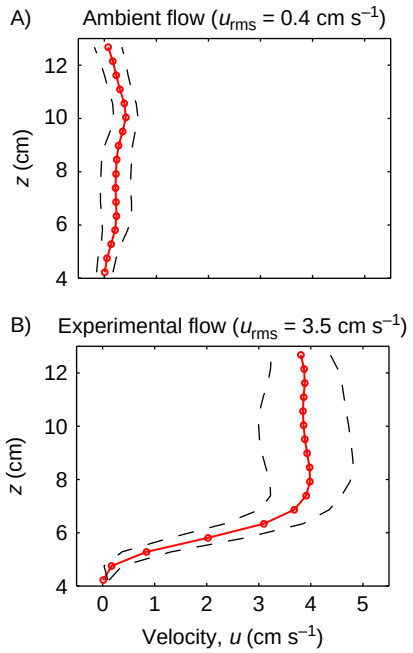

Fig. 3 Mean water velocity profiles (red) relative to the surface of the substratum in ambient (A) and experimental (B) flow conditions. Vertical profiles were extracted from the DPIV data at the horizontal position $x = 11.6$ cm. Velocity was measured over 14.3 s in ambient flow and 21.0 s in experimental flow. The dashed lines show the standard deviation of the mean velocity.

Table 2 Ostracod swimming speeds and trajectories (mean ± SD). The observed ostracod velocity is the vector sum of the ostracod swimming velocity and the local fluid velocity. Relative swimming velocity was calculated by subtracting the local velocity vector from the ostracod velocity vector at each time step, and passive velocity is the velocity at which a neutrally buoyant particle following the flow would travel. Mean speeds were calculated from the velocity vectors. A low net:gross displacement ratio (NGDR) indicates a trajectory with a high degree of tortuosity.

		Speed (cm s^{-1})			NGDR	
Flow condition	No. tracks	Observed	Relative	Passive	Observed	Passive
Ambient	22	4.3 ± 2.3	4.3 ± 2.3	0.36 ± 0.2	0.5 ± 0.3	0.7 ± 0.3
Experimental	28	5.0 ± 2.3	4.2 ± 1.7	1.0 ± 0.02	0.7 ± 0.2	1.0 ± 0.02

ment, shear rates were much higher in the boundary layer (Table 1, Fig. 2H).

[14] Vertical profiles of the mean horizontal velocities for the two flow treatments are shown in Fig. 3. Local velocities at any height above the substratum varied in direction in the ambient flow condition (Fig. 3A), so the mean horizontal velocity profile was variable. There was a small increase in velocity with distance above the substratum, and the logarithmic portion of the velocity profile was defined as the first five points above the substratum where velocity increased. In contrast, the experimental flow treatment (Fig. 3B) had a logarithmic velocity profile typical of boundary layer flows (Nowell and Jumars 1984). The boundary shear velocity, u_*, in the experimental flow treatment (1.11 cm s^{-1}; $R^2 = 0.95$; $p < 0.01$; $n = 5$) was approximately 29% of the mean free-stream flow, u_0, and was substantially higher than the u_* in the ambient condition (0.04 cm s^{-1}; $R^2 = 0.95$; $p < 0.001$; $n = 6$), which was approximately 12% of u_0 (Table 1).

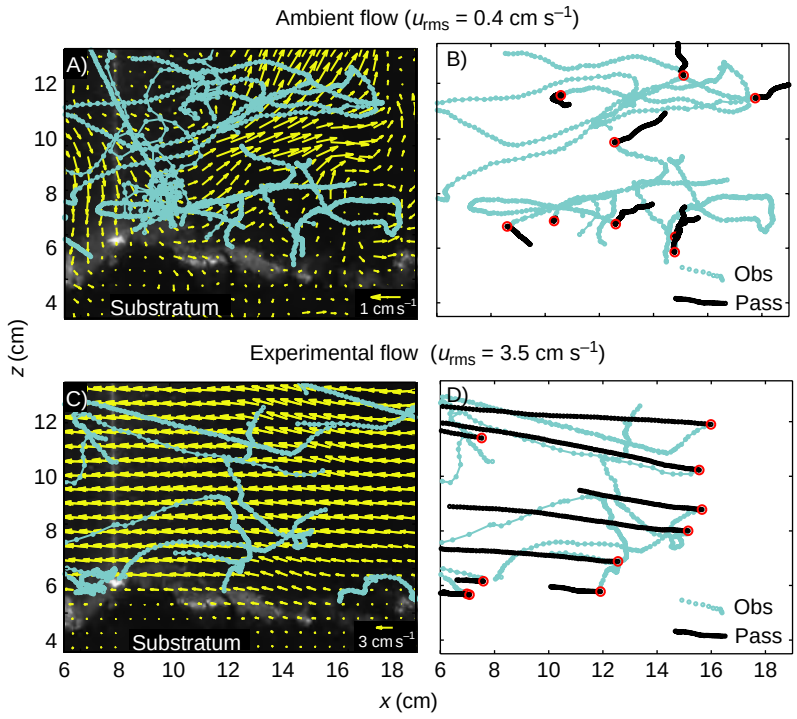

Fig. 4 Representative ostracod swimming tracks. Observed ostracod tracks (blue), instantaneous fluid velocity vectors (yellow arrows), and background benthic community are shown in ambient (A–B; $n = 13$) and experimental flow conditions (C–D; $n = 14$). Passive tracks of neutrally buoyant particles (black) advected from the same initial starting points (red circles) as the ostracods are shown along with the observed ostracod tracks (blue) in ambient ($n = 9$) and experimental flow conditions ($n = 9$). The neutrally buoyant particles were followed through the measured field flow data for the same number of time steps as the ostracods that started at the same points in the flow field. Some of the tracks have been omitted for clarity.

Swimming Behavior

[15] A total of 22 tracks of different individual ostracods were digitized in the ambient flow treatment, and the mean path time was 2.9 ± 1.8 s. A total of 28 tracks were digitized in the experimental flow treatment, and the mean path time was 2.0 ± 1.1 s. Mean relative swimming speeds were similar in the two treatments, but tracks were straighter (less tortuous) in the experimental flow treatment ($t_{48} = -3.24$, $p = 0.002$; Table 2, Fig. 4). Tracks of passive, neutrally buoyant particles with the same initial starting positions as the ostracods were different from the ostracod tracks (Fig. 4B, D). The passive particles moved at mean speeds significantly slower than the observed ostracod velocities in both treatments, indicating that active swimming is important for ostracod transport

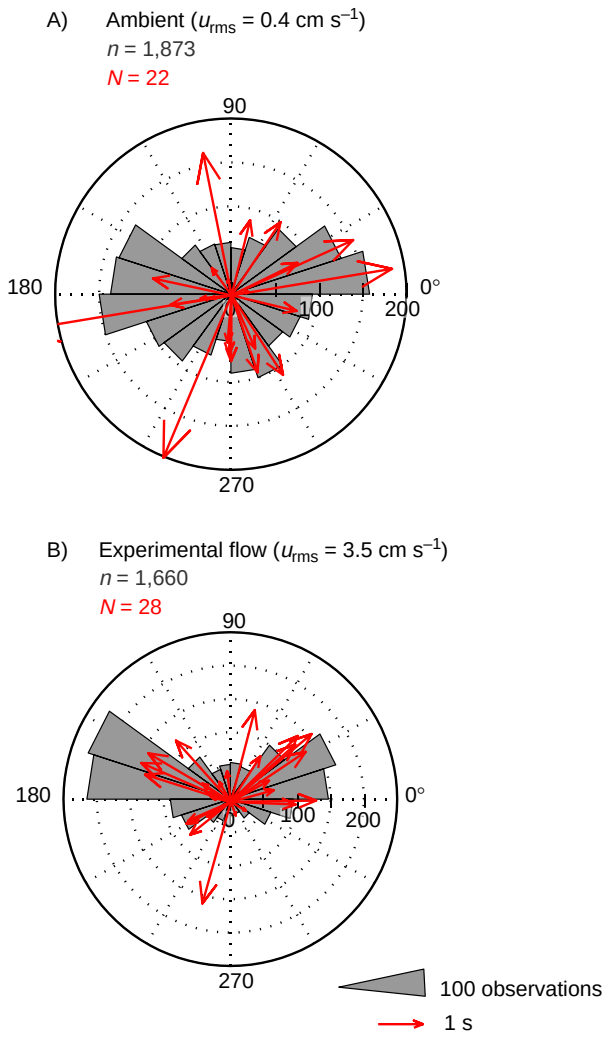

Fig. 5 Ostracod swimming angles in ambient and experimental flow after subtracting local fluid velocities. Angles of 0 and 180° indicate horizontal swimming (along the *x*-axis), and angles of 90° and 270° indicate vertical swimming (along the *z*-axis). A circular frequency histogram of instantaneous angles pooled for all individuals, *n*, is shown in gray, and a compass plot of mean direction and track time length for each individual, *N*, is shown in red.

(Table 2; ambient: $t_{42} = -8.30$, $p < 0.001$; experimental: $t_{54} = -9.43$, $p < 0.001$). The tracks of passive particles also had a significantly higher NGDR (i.e., were straighter) in both treatments (Table 2; ambient: $t_{42} = 2.03$, $p = 0.049$; experimental: $t_{54} = 6.71$, $p < 0.001$).

[16] In the ambient flow treatment, instantaneous swimming angles were uniformly distributed ($z = 1.41$, $n = 1873$, $p = 0.24$), indicating that swimming direction was random. In contrast, in the experimental flow treatment, instantaneous angles were nonuniform ($z = 59.18$, $n = 1662$, $p < 0.001$) and tended to be oriented parallel to the benthos (Fig. 5). The distributions of the orientations of the mean swimming angles for each track were uniform in both treatments (ambient: $z = 0.07$, $n = 22$, $p = 0.91$; experimental: $z = 1.20$, $n = 28$, $p < 0.30$).

[17] There was no difference in the number of interactions between ostracods and the benthos between the two treatments ($\chi^2_1 = 0.91$, $p = 0.34$). Similarly, there was no difference in numbers of interactions between ostracods and conspecifics between the two treatments ($\chi^2_1 = 3.8 \times 10^{-4}$, $p = 0.99$). However, there was a relationship between height above the benthos and interactions with conspecifics: interactions occurred more frequently in the boundary layer in experimental flow ($\chi^2_1 = 6.16$, $p = 0.013$; Table 3), and the mean *z*-position of the interactions was closer to the benthos in experimental flow compared to ambient flow (Mann–Whitney $U = 106$, $p = 0.02$; Fig. 6).

Discussion

[18] Under natural field conditions, freely swimming plankton moving between the benthos and the water column face a range of water motions. At higher flow speeds in particular, shear rates are enhanced and flow may be more variable. Our results show that in situ trajectories of the ostracod *Paravargula trifax*, including tortuosity of swimming trajectories, swimming angle, and interactions with conspecifics, are influenced by local water flow (i.e., within centimeters of the organism).

Table 3 The number (and proportion) of ostracod interactions with conspecifics in the experimental flow treatment within the boundary layer and in the free-stream flow. Each track was divided into 0.5-s intervals, and categories correspond to numbers of interactions based on counts in each interval.

	Number of interactions with conspecifics		
Location	**0**	**1 or 2**	**Total**
Free-stream ($z > 9$ cm)	46 (0.94)	3 (0.06)	49
Boundary layer ($z < 9$ cm)	39 (0.74)	14 (0.26)	53

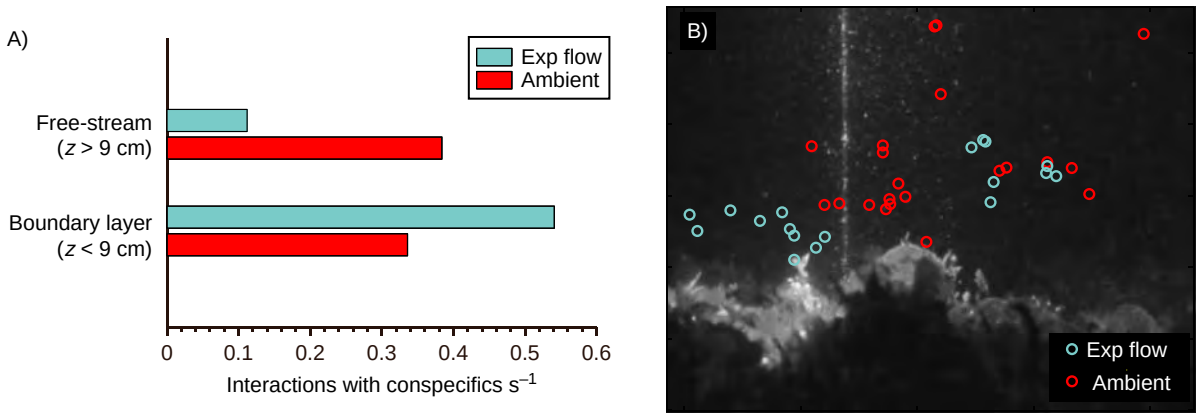

Fig. 6 Frequency (A) and location (B) of ostracod interactions with conspecifics within and above the benthic boundary layer for ambient and experimental flow conditions.

In Situ Flow Measurements

[19] Studies of plankton conducted in still water in laboratory tanks have provided important insight about individual behavioral responses to controlled environmental parameters but may not accurately reflect swimming trajectories in the field. The use of new tools for simultaneous measurements of organism-scale environmental flow and animal trajectories used in this study and elsewhere (Gallager et al. 2004; Sheng et al. 2006) make it possible to quantify swimming behavior in the natural environment. An advantage of the relatively portable SCUVA compared to other in situ DPIV techniques (Doron et al. 2001; Liao et al. 2009) is that it enables field measurements in shallow water near delicate benthic communities in habitats with complex terrain (e.g., coral reefs, under docks). These types of measurements, in conjunction with laboratory and modeling studies, provide a more comprehensive understanding of the interaction of plankton swimming behaviors with the fluid environment.

[20] Our results suggest that boundary shear velocities (u_*) over rugose benthic communities living on substrata of finite size in natural habitats can be higher than those measured in fully developed boundary layers over relatively smooth substrata in laboratory flumes or in flat, soft-substratum field sites. For example, the boundary shear velocity in our experimental flow treatment was higher than u_* values measured in laboratory flumes (e.g., Pawlik and Butman 1993; Weissburg and Zimmer-Faust 1993; Reidenbach et al. 2010) and in the field (e.g., Grant et al. 1984) at comparable free-stream velocities. One reason for this difference is that, as a fluid flows across a structure, the boundary layer thickens with distance from the upstream edge of the structure. Therefore organisms living on objects such as docks, ships, rocks, or coral heads encounter boundary layers that are not fully developed (e.g., Koehl 2007). Not only do boundary layers grow with distance from a leading edge, but they also grow over time. Therefore, in shallow habitats characterized by changing flow directions due to waves, boundary layers are thinner than they are in steady unidirectional flow at comparable instantaneous free-stream velocities (e.g., Denny 1988). In the present study, the boundary layer may not have been fully developed because the measurements were made at a distance of only 2 m from the leading edge of the dock (local Reynolds number, $\mathrm{Re}_x \approx x u_{\mathrm{rms}}/\nu \sim 7 \times 10^4$, where ν is the kinematic viscosity and where $\mathrm{Re}_x \sim 3\text{–}5 \times 10^5$ is transitional on a flat plate). Furthermore, in the experimental flow treatment, although we made all our measurements during periods when the free-stream flow relative to the dock had reached a steady velocity, the boundary layer had to develop anew each time that we started pulling the dock through the water. These factors, along with the high degree of rugosity of the fouling community, which can raise the turbulence in

the boundary layer and hence increase u_* (reviewed in Koehl 2007), likely contributed to the elevated u_* values we measured.

Swimming Trajectories and Orientation

[21] The faster the water flow, the greater the effect on ostracod trajectories. In the experimental flow treatment, which was characterized by higher shear than the ambient flow condition (Table 1, Fig. 2), ostracods had straighter trajectories that were more parallel to the benthos and the direction of flow than they were in the slower ambient flow. These observations indicate that ostracod maneuverability was diminished and passive transport was more important in the faster water flow treatment (Table 2, Figs. 4, 5). Field studies of another myodocopid ostracod, *Vargula annecohenae*, with a higher mean swimming speed (approx. 8 cm s^{-1}; Rivers and Morin 2008) showed that they were less abundant in the water column when current speeds at the top of the water column exceeded 25 cm s^{-1}, suggesting diminished foraging activity in more rapid flow (Gerrish et al. 2009). Because Gerrish et al. (2009) did not measure water velocities in the benthic boundary layer, we cannot directly compare our experimental flow condition (mean u_{rms} of 3.49 cm s^{-1}) that altered ostracod behavior with the water motion that caused ostracods to stop swimming in their study. However, assuming that $u^* \sim 0.1\ u_0$ (typical for well-behaved flows), then $u^* \sim$ 2.5 cm s^{-1}, which is the same order of magnitude as the experimental flow treatment in the present study. Since water flows across benthic communities in the field, the swimming activities of ostracods and other freely swimming plankton associating with the benthos are probably frequently influenced by local flows.

[22] The effect of water flow on observed trajectories can strongly depend on species-specific behaviors. For example, in three different copepod species the observed NGDR in background turbulence was tied to size and swimming style of each species, and in the largest species, *Calanus finmarchicus*, tracks became *more* tortuous in turbulence (Yen et al. 2008). The motility number, Mn, which is the ratio of observed swimming velocity to the root mean square of the turbulent velocities (Gallager et al. 2004), can be used to estimate the relative importance of swimming behavior and background flow. Mn $>$ 1 suggests that behavior exceeds turbulence, and Gallager et al. (2004) found that Mn $>$ 3 was required for zooplankton to aggregate. In the present study, the Mn was approximately 30 in the ambient flow and approximately 8 in the experimental flow, suggesting that behavior dominated over physical forcing. However, the ostracods in the experimental flow experienced a mean steady velocity in addition to turbulent velocities, which likely influenced the trajectories. The trajectories of zooplankton with slower swimming speeds, such as the myodocopid ostracod *Cylindroleberis mariae* (maximum speed approx. 2 cm s^{-1}; Corbari et al. 2005), would be expected to be even more vulnerable to moving fluid.

[23] Although ostracod trajectories were affected by environmental flow, several lines of evidence indicate that the active behaviors of these animals also affect their paths. In both flow treatments, ostracod tracks were more tortuous than were tracks of passive, neutrally buoyant particles. This suggests that even in the experimental flow treatment, ostracods still had some control over swimming paths (Table 2, Fig. 4). Mean swimming speeds relative to the surrounding water were the same in the two treatments, indicating that biological propulsive capability was not affected (Table 2). The finding that ostracods moved at a mean speed that was 5-fold faster than that of modeled passive particles in the ambient flow condition and 10-fold faster in the experimental flow treatment (Table 2) further supports the idea that swimming behavior dominates background flow to determine the position of the ostracods.

Interactions with Benthos and with Conspecifics

[24] Among ostracod species, which are primarily associated with the benthos, swimming plays an important role in both feeding and mating activities. Myodocopid ostracods consume a wide array of food items, feeding on detritus and living and dead animal material in the benthos by grasping and scraping with the feeding appendages (Vannier et al. 1998). The ability to maneuver while swimming in water flowing near the substratum is likely important for accessing different sites in the benthic community. Although the number of interactions with the benthos was similar in our two flow treatments, in the experimental flow condition the ob-

served ostracod trajectories (due to the vector sums of the instantaneous ostracod swimming velocity and the local fluid velocity) were much straighter, and swimming angles were parallel to the substratum and the direction of water flow. These observations suggest that in faster flow, ostracods are swept past the benthos by the flowing water and thus may have less control over the locations of contact with the benthos than they do in slower flow (Figs. 3, 4).

[25] Copulatory displays in myodocopid ostracods occur in the water column; thus, it is plausible that these activities are altered in the presence of water flow in the environment. To our knowledge, only one set of studies has examined the swimming behavior of mating ostracods (Rivers and Morin 2008, 2009). Laboratory work with luminescent ostracods from the Caribbean (*Vargula annecohenae*) showed that males swam upward in a helical pattern during courtship to attract females, and these swim paths were accompanied by a characteristic, luminescent signaling pattern. Mature females followed the paths of the males, but it is not known whether copulation occurred in the water column. The species in our study, *Paravargula trifax*, is not luminescent and did not swim in a helical pattern. However, it is possible that courtship and copulation occur in the water column and, therefore, frequency of interactions with conspecifics in the water column might correlate with enhanced reproductive success. Although there was no difference in interactions with other ostracods between our two flow treatments, further examination showed that in the experimental flow treatment, these interactions were primarily confined to the boundary layer within 9 cm from the substratum (Fig. 6). This is somewhat surprising given that shear is most pronounced close to the substratum (Fig. 1, Table 1) and that strong velocity gradients have been shown to interfere with mechanosensory detection of other organisms by copepods (e.g., Robinson et al. 2007). On the other hand, quiescent microhabitats in the lee of sessile organisms living on the substratum may provide a refuge where flow speeds and shear are diminished and ostracod interactions can occur. However, the data from this study do not show strong evidence of interactions corresponding with areas of low flow (Fig. 6B), so the mechanism behind enhanced interactions in the benthic boundary layer is unknown.

Plankton Behavior at the Benthic Boundary Layer and Ecological Roles

[26] Many of the studies of the movement of small animals in the benthic boundary layer focus on recruitment and metamorphosis of meroplanktonic larvae (e.g., Butman et al. 1988; Fuchs et al. 2004; Koehl 2007). In contrast to these meroplanktonic larvae of benthic invertebrates, which need to move through the benthic boundary layer only during settlement, ostracods and other freely swimming demersal holoplankton move through this layer frequently. Therefore, it might be expected that demersal zooplankton and settling larvae respond to environmental flow in different ways. Meroplankton are typically smaller (hundreds of micrometers) and slower (swimming velocities of approx. $0.1–1.0\ \mathrm{cm\ s^{-1}}$; Chia et al. 1984) than are demersal zooplankton like ostracods and thus are more likely to be overwhelmed by environmental flow (although active swimming continues in high shear for some species of larvae; Jonsson et al. 1991). In contrast, holoplanktonic copepods exhibit countercurrent swimming in flow velocities up to $3\ \mathrm{cm\ s^{-1}}$ (Shang et al. 2008). Larvae respond to fluid mechanical disturbances by ceasing to swim and sinking (e.g., polychaete larvae: Pawlik and Butman 1993; gastropod larvae: Fuchs et al. 2004), whereas various types of holoplankton respond by escape jumping (e.g., copepods: Fields and Yen 1997; Kiørboe et al. 1999; ciliates: Jakobsen 2001). These different responses might help explain differences in the vertical distribution of meroplankton and holoplankton over the sea bed (Holzman et al. 2005). Further studies of the swimming behaviors of both meroplanktonic larvae and demersal holoplankton in realistic environmental flows at ecologically relevant scales will enhance our understanding of how individual responses to the fluid environment correspond to population and community patterns.

Significance to Aquatic Environments

[27] Organisms that live within the benthic boundary layer play a critical role in benthic–pelagic coupling

(e.g., the cycling of organic material) not only by their own foraging activities and movement between the water column and the substratum but also by being prey for benthic animals. Water flow influences prey capture rates and selectivity by benthic planktivores (reviewed by Wildish and Kristmanson 1997), not only by increasing transport of plankton to the capture structures of sessile predators but also by reducing the ability of predators to hold on to captured prey (e.g., Shimeta and Koehl 1997). In addition, the velocity and shear fluctuations in turbulent flow can interfere with the ability of planktonic animals with escape responses (e.g., copepods) to detect the fluid signals of benthic predators and thus can increase rates of predation (Robinson et al. 2007). Because the turbulent flow environment near the substratum is dynamic and spatially variable (reviewed by Nowell and Jumars 1984; Koehl 2007; Reidenbach et al., 2009), simultaneous measurements of instantaneous local flow velocities and behaviors of planktonic organisms can provide insights about the mechanisms responsible for the effects of environmental water flow on their ecological interactions.

[28] In the study reported here, crustacean plankton in the benthic boundary layer were not simply transported like passive particles by the flow. Nonetheless, their behavior was altered by moving water, and these flow-induced changes in their trajectories may affect mating, foraging, and encounters with benthic predators. The interaction between plankton behavior and water flow suggests that flow plays an important role in structuring vertical distributions of coexistent demersal plankton species; plankton species may inhabit a particular height above the substratum based on benefits associated with a particular flow regime.

Acknowledgments We are grateful to the suggestions of three anonymous reviewers, which substantially improved the manuscript. We thank L. Kornicker at the Smithsonian for ostracod species identification, T. Cooper for field and data processing assistance, and M. Hadfield and F. Thomas for the use of facilities at the University of Hawaii Kewalo Marine Lab and Hawaii Institute of Marine Biology, respectively. This research was supported by the National Science Foundation (IOS-0842681 to M.A.R.K.) and the Office of Naval Research (N000141010137 to J.O.D.).

References

Adrian, R. J. 1991. Particle-imaging techniques for experimental fluid-mechanics. Annu. Rev. Fluid Mech. **23**: 261–304, doi:10.1146/annurev.fl.23.010191.001401.

Butman, C. A., J. P. Grassle, and C. M. Webb. 1988. Substrate choices made by marine larvae settling in still water and in a flume flow. Nature **333**: 771–773, doi:10.1038/333771a0.

Chia, F.-S., J. Buckland-Nicks, and C. M. Young. 1984. Locomotion of marine invertebrate larvae. Can. J. Zool. **62**: 1205–1222, doi:10.1139/z84-176.

Corbari, L., P. Carbonel, and J. Massabuau. 2005. The early life history of tissue oxygenation in crustaceans: The strategy of the myodocopid ostracod *Cylindroleberis mariae*. J. Exp. Biol. **208**: 661–670, doi:10.1242/jeb.01427.

Denny, M. W. 1988. Biology and Mechanics of the Wave-Swept Environment. Princeton Univ. Press.

Dicke, M., and P. A. Burrough. 1988. Using fractal dimensions for characterizing tortuosity of animal trails. Physiol. Entomol. **13**: 393–398, doi:10.1111/j.1365-3032.1988.tb01122.x.

Doron, P., L. Bertuccioli, J. Katz, and T. R. Osborn. 2001. Turbulence characteristics and dissipation estimates in the coastal ocean bottom boundary layer from PIV data. J. Phys. Oceanogr. **31**: 2108–2134, doi:10.1175/1520-0485(2001)031<2108:TCADEI>2.0.CO;2.

Fields, D. M., and J. Yen. 1997. The escape behavior of marine copepods in response to a quantifiable fluid mechanical disturbance. J. Plankton Res. **19**: 1289–1304, doi:10.1093/plankt/19.9.1289.

Fuchs, H. L., L. S. Mullineaux, and A. R. Solow. 2004. Sinking behavior of gastropod larvae (*Ilyanassa obsoleta*) in turbulence. Limnol. Oceanogr. **49**: 1937–1948, doi:10.4319/lo.2004.49.6.1937.

Gallager, S. M., H. Yamazaki, and C. S. Davis. 2004. Contribution of fine-scale vertical structure and swimming behavior to formation of plankton layers on Georges Bank. Mar. Ecol. Prog. Ser. **267**: 27–43, doi:10.3354/meps267027.

Gerrish, G. A., J. G. Morin, T. J. Rivers, and Z. Patrawala. 2009. Darkness as an ecological resource: The role of light in partitioning the nocturnal niche. Oecologia **160**: 525–536, doi:10.1007/s00442-009-1327-8.

Grant, W. D., A. J. Williams, and S. M. Glenn. 1984. Bottom stress estimates and their prediction on the northern California continental shelf during CODE-1: The importance of wave-current interaction. J. Phys. Oceanogr. **14**: 506–527, doi:10.1175/1520-0485(1984)014<0506:BSEATP>2.0.CO;2.

Holzman, R., M. A. Reidenbach, S. G. Monismith, J. R. Koseff, and A. Genin. 2005. Near-bottom depletion of zooplankton over a coral reef—II: Relationships with zooplankton swimming ability. Coral Reefs. **24**: 87–94, doi:10.1007/s00338-004-0450-6.

Irigoien, X., R. P. Harris, and R. N. Head. 2000. Does turbulence play a role in feeding and reproduction of *Calanus finmarchicus*? J. Plankton Res. **22**: 399–407, doi:10.1093/plankt/22.2.399.

Jakobsen, H. H. 2001. Escape response of planktonic protists to fluid mechanical signals. Mar. Ecol. Prog. Ser. **214**: 67–78, doi:10.3354/meps214067.

Jonsson, P. R., C. Andre, and M. Lindegarth. 1991. Swimming behavior of marine bivalve larvae in a flume boundary-layer flow: Evidence for near-bottom confinement. Mar. Ecol. Prog. Ser. **79**: 67–76, doi:10.3354/meps079067.

Katija, K., and J. O. Dabiri. 2008. In situ field measurements of aquatic animal-fluid interactions using a self-contained underwater velocimetry apparatus (SCUVA). Limnol. Oceanogr. Methods **6**: 162–171, doi:10.4319/lom.2008.6.162.

Kiørboe, T., E. Saiz, and A. Visser. 1999. Hydrodynamic signal perception in the copepod *Acartia tonsa*. Mar. Ecol. Prog. Ser. **179**: 97–111, doi:10.3354/meps179097.

Koehl, M. A. R. 2007. Mini review: Hydrodynamics of larval settlement into fouling communities. Biofouling **23**: 357–368, doi:10.1080/08927010701492250.

Koehl, M. A. R., J. A. Strother, M. A. Reidenbach, J. R. Koseff, and M. G. Hadfield. 2007. Individual-based model of larval transport to coral reefs in turbulent, wave-driven flow: Behavioral responses to dissolved settlement inducer. Mar. Ecol. Prog. Ser. **335**: 1–18, doi:10.3354/meps335001.

Liao, Q., H. A. Bootsma, J. E. Xiao, J. V. Klump, A. Hume, M. H. Long, and P. Berg. 2009. Development of an in situ underwater particle image velocimetry (UWPIV) system. Limnol. Oceanogr. Methods **7**: 169–184, doi:10.4319/lom.2009.7.169.

Marcus, N. H., and F. Boero. 1998. Minireview: The importance of benthic-pelagic coupling and the forgotten role of life cycles in coastal aquatic systems. Limnol. Oceanogr. **43**: 763–768, doi:10.4319/lo.1998.43.5.0763.

Nowell, A. R. M., and P. A. Jumars. 1984. Flow environments of aquatic benthos. Annu. Rev. Ecol. Syst. **15**: 303–328, doi:10.1146/annurev.es.15.110184.001511.

Pawlik, J. R., and C. A. Butman. 1993. Settlement of a marine tube worm as a function of current velocity: Interacting effects of hydrodynamics and behavior. Limnol. Oceanogr. **38**: 1730–1740, doi:10.4319/lo.1993.38.8.1730.

Reidenbach, M. A., J. R. Koseff, and M. A. R. Koehl. 2009. Hydrodynamic forces on larvae affect their settlement on coral reefs in turbulent, wave-driven flow. Limnol. Oceanogr. **54**: 318–330, doi:10.4319/lo.2009.54.1.0318.

Reidenbach, M. A., M. Limm, M. Hondzo, and M. T. Stacey. 2010. Effects of bed roughness on boundary layer mixing and mass flux across the sediment-water interface. Water Resour. Res. **46**: W07530, doi:10.1029/2009WR008248.

Rivers, T. J., and J. G. Morin. 2008. Complex sexual courtship displays by luminescent male marine ostracods. J. Exp. Biol. **211**: 2252–2262, doi:10.1242/jeb.011130.

———. 2009. Plasticity of male mating behaviour in a marine bioluminescent ostracod in both time and space. Anim. Behav. **78**: 723–734, doi:10.1016/j.anbehav.2009.06.020.

Robinson, H. E., C. M. Finelli, and E. J. Buskey. 2007. The turbulent life of copepods: Effects of water flow over a coral reef on their ability to detect and evade predators. Mar. Ecol. Prog. Ser. **349**: 171–181, doi:10.3354/meps07123.

Saiz, E., and T. Kiørboe. 1995. Predatory and suspension-feeding of the copepod *Acartia tonsa* in turbulent environments. Mar. Ecol. Prog. Ser. **122**: 147–158, doi:10.3354/meps122147.

Shang, X., G. H. Wang, and S. J. Li. 2008. Resisting flow—laboratory study of rheotaxis of the estuarine copepod *Pseudodiaptomus annandalei*. Mar. Freshwat. Behav. Physiol. **41**: 109–124, doi:10.1080/10236240801905859.

Sheng, J., E. Malkiel, and J. Katz. 2006. Digital holographic microscope for measuring three-dimensional particle distributions and motions. Appl. Opt. **45**: 3893–3901, doi:10.1364/AO.45.003893.

Shimeta, J., and M. A. R. Koehl. 1997. Mechanisms of particle selection by tentaculate suspension feeders during encounter, retention, and handling. J. Exp. Mar. Biol. Ecol. **209**: 47–73, doi:10.1016/S0022-0981(96)02684-6.

Vannier, J., K. Abe, and K. Ikuta. 1998. Feeding in myodocopid ostracods: Functional morphology and laboratory observations from videos. Mar. Biol. **132**: 391–408, doi:10.1007/s002270050406.

Weissburg, M. J., and R. K. Zimmer-Faust. 1993. Life and death in moving fluids: Hydrodynamic effects of chemosensory-mediated predation. Ecology **74**: 1428–1443, doi:10.2307/1940072.

Wildish, D., and D. Kristmanson. 1997. Benthic Suspension Feeders and Flow. Cambridge Univ. Press.

Willert, C. E., and M. Gharib. 1991. Digital particle image velocimetry. Exp. Fluids **10**: 181–193, doi:10.1007/BF00190388.

Williams, T. A. 1994. A model of rowing propulsion and the ontogeny of locomotion in *Artemia* larvae. Biol. Bull. **187**: 164–173, doi:10.2307/1542239.

Woodson, C. B., D. R. Webster, M. J. Weissburg, and J. Yen. 2005. Response of copepods to physical gradients associated with structure in the ocean. Limnol. Oceanogr. **50**: 1552–1564, doi:10.4319/lo.2005.50.5.1552.

Yen, J., K. D. Rasberry, and D. R. Webster. 2008. Quantifying copepod kinematics in a laboratory turbulence apparatus. J. Mar. Syst. **69**: 283–294, doi:10.1016/j.jmarsys.2006.02.014.

Zar, J. H. 1999. Biostatistical Analysis. 4th ed. Prentice-Hall.

Zaret, R. E., and W. C. Kerfoot. 1980. Shape and swimming technique of *Bosmina longirostris*. Limnol. Oceanogr. **25**: 126–133, doi:10.4319/lo.1980.25.1.0126.

Received: 7 March 2011
Amended: 13 June 2011
Accepted: 23 July 2011